SERBIAN JOURNAL OF ELECTRICAL ENGINEERING
Vol. 11, No. 4 (special issue), December 2014, 701-717

UDC: 537.622.4: 519.61/.64 **DOI: 10.2298/SJEE1404701J**

Magnetic Field of Rectangular Current Loop with Sides Parallel and Perpendicular to the Surface of High-permeability Material

Anamarija Juhas[1], Neda Pekarić-Nađ[1], Hannes Toepfer[2]

Abstract: In this paper, method of current images is used to calculate magnetic field of a rectangular loop in presence of high-permeability material. We provide closed form description for the images of the current loop placed between two semi-infinite blocks of high-permeability material, in the cases when the plane of the loop is parallel or perpendicular to the surfaces of blocks. A case study of using the method of images to calculate magnetic field of rectangular loop inside cube made of high-permeability material is also provided.

Keywords: Method of images, Magnetic field, Magnetostatics.

1 Introduction

Method of images was first introduced in nineteenth century by Lord Kelvin in the course of solving electrostatic problems [1]. Lord Kelvin was followed by Maxwell, who enlarged the application of the method to a list of problems concerning combinations of equipotential spheres and planes in presence of electric charges [2, 3]. The application of the method of images is later extended to numerous problems in magnetostatics (see e.g. [3]).

Using the method of current images, Roshen investigated effects of semi-infinite magnetic substrate on planar inductors [4] and effects of magnetic substrate of finite thickness on planar inductors [5]. He also studied planar inductors sandwiched between two semi-infinite magnetic substrates [6].

For bio-magnetic experiments in *in vitro* studies, concerning effects of extremely low frequency magnetic field on biological material, a high-precision exposure system is needed (see e.g. [7, 8]). The exposure systems are usually based on systems of coaxial coils placed in a box of high-conductivity and/or high-permeability material (see e.g. [7]). The box represents either commercial incubator or high-permeability enclosure for shielding background magnetic field. The system of the coils should be designed to generate linearly polarized magnetic field of high uniformity in specified volume. In order to calculate

[1]Faculty of Technical Sciences, University of Novi Sad, Serbia; E-mails: ajuhas@uns.ac.rs; pekaric@uns.ac.rs
[2]Technische Universität, University of Ilmenau, Germany; E-mail: hannes.toepfer@tu-ilmenau.de

magnetic field inside the coils the effects of the box must be included. In [7] the effects of $\mu-$ metal enclosure on magnetic field are modelled using 26 closest images.

Although the method of current images has a long history, it is still developing for the problems that include AC currents and boundaries of complex shapes [9].

In Section 2 we provide brief overview of the current images for a rectangular loop with sides parallel and/or perpendicular to the surface of a semi-infinite block of high-permeability material. The current images of the rectangular loop sandwiched between two semi-infinite high-permeability blocks, in the cases when i) the plane of the loop is parallel to the surfaces of blocks and ii) the plane of the loop is perpendicular to the surfaces of blocks are also considered, along with discussion of the number of images which is sufficient to approximate magnetic field in the air between blocks. A case study of the current loop in cube made of high-permeability material is provided in Section 3.

2 Current Images of Rectangular Loop

In this section we provide brief overview of the current images for the rectangular loop, in the cases when the plane of the loop is parallel or perpendicular to the surface of semi-infinite block of high-permeability material (Subsection 2.1). The current images of the rectangular loop sandwiched between two semi-infinite high-permeability blocks, in the cases when the plane of the loop is parallel (Subsection 2.2) or perpendicular (Subsection 2.3) to the surfaces of blocks are also provided. We also discuss the number of the current images which is sufficient to approximate magnetic field in the air (between two blocks).

Without loss of generality we can assume that sides of the rectangular loop are parallel to $x-$ and $y-$axis and the center of the loop is at the origin, as shown in Fig. 1.

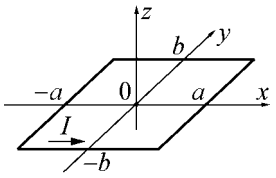

Fig. 1 – *Rectangular current loop*.

In this paper only images that describe the effects of high-permeability material on magnetic field in the air are considered. In what follows, we assume

that the high-permeability material has constant permeability $\mu = \mu_r \mu_0$, where μ_r is relative permeability and $\mu_0 = 4\pi \cdot 10^{-7}$ H/m.

2.1 Plane of the loop parallel or perpendicular to the surface of high-permeability material

Let us first assume that a semi-infinite block of high-permeability material occupies the region $z \le z_m$, where $z_m < 0$ (the surface of the material is in the plane $z = z_m$).

The application of the method of current images allows calculation of magnetic flux density vector in the air as there is homogeneous medium of permeability μ_0. According to the method of images, magnetic flux density vector in the air (for $z > z_m$) can be calculated by introducing the image of the considered loop (see e.g. [4, 9]). Let us denote parameter

$$\alpha = \frac{\mu_r - 1}{\mu_r + 1}. \tag{1}$$

The image of the loop is placed in the plane $z = 2z_m$ and the current in the image loop is equal to αI in respect to the reference direction of the current in the original loop (see Fig. 2). In what follows we will assume that the reference directions of the current in the original loop and all image loops are the same.

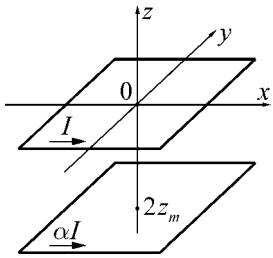

Fig. 2 – *Rectangular loop and its image in the plane* $z = 2z_m$.

Now let us assume that the semi-infinite block of high-permeability material occupies the region $x \le x_m$, where $x_m < -a$ (the surface of material is in the plane $x = x_m$). The magnetic flux density vector in the air (for $x > x_m$) can be obtained by removing the block and introducing the image of the considered loop. In this case, the center of the image loop is at point with coordinates $(2x_m, 0, 0)$ and the current in the image loop is equal to $-\alpha I$, as illustrated in Fig. 3.

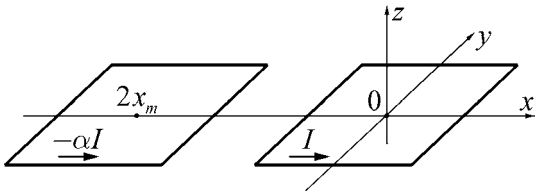

Fig. 3 – *Rectangular loop and its image with center at* $(2x_m, 0, 0)$.

2.2 Plane of the loop parallel to the surfaces of two blocks of high-permeability material

In this subsection we consider a rectangular loop sandwiched between two semi-infinite blocks of high-permeability material, where one block occupies the region $z \le z_{\text{bottom}} < 0$ and the other the region $z \ge z_{\text{top}} > 0$. The loop is in the plane $z = 0$ and hence it is parallel to the surfaces of both blocks. Cross-section of the considered system is presented in Fig. 4.

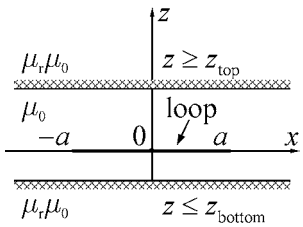

Fig. 4 – *Rectangular loop sandwiched between two blocks* $z \le z_{\text{bottom}} < 0$ *and* $z \ge z_{\text{top}} > 0$.

As in previous subsection, the method of current images can be used to model the influence of both high-permeability blocks on magnetic field (see e.g. [6]). The images form an infinite series and we say that the images are of $(k+1)$st order when they are "images" of kth order images in respect to the planes $z = z_{\text{bottom}}$ and $z = z_{\text{top}}$. It is easy to see that there are two images of the first order, placed in the planes $z_1' = 2z_{\text{top}}$ and $z_1'' = 2z_{\text{bottom}}$, both having current αI (in respect to the same reference direction as in the original loop).

The following proposition describes the images of kth order, $k \ge 1$, for the system presented in Fig. 4.

Proposition 1. For the system presented in Fig. 4, there are two images of kth order, $k \ge 1$, both with current $\alpha^k I$ and parallel to the original loop with centers on z – axis, placed in the planes

$$z'_k = 2\left(\left\lfloor \frac{k+1}{2} \right\rfloor z_{\text{top}} - \left\lfloor \frac{k}{2} \right\rfloor z_{\text{bottom}}\right), \tag{2}$$

and

$$z''_k = 2\left(\left\lfloor \frac{k+1}{2} \right\rfloor z_{\text{bottom}} - \left\lfloor \frac{k}{2} \right\rfloor z_{\text{top}}\right), \tag{3}$$

where $\lfloor u \rfloor$ denotes largest integer not greater than u.

Proof. Mathematical induction is used to prove Proposition 1. Both (2) and (3) obviously hold for $k=1$. Let us assume that they also hold for some value of k. Then the images of $(k+1)$st order have currents $\alpha^{(k+1)}I$ and they are placed at the planes $z'_{k+1} = 2z_{\text{bottom}} - z'_k$ and $z''_{k+1} = 2z_{\text{top}} - z''_k$. Substituting (2) – (3) into z'_{k+1} and z''_{k+1} and taking into account that

$$1 + \left\lfloor \frac{k}{2} \right\rfloor = \left\lfloor \frac{k+2}{2} \right\rfloor,$$

we obtain

$$z'_{k+1} = 2\left(\left\lfloor \frac{k+2}{2} \right\rfloor z_{\text{top}} - \left\lfloor \frac{k+1}{2} \right\rfloor z_{\text{bottom}}\right),$$

$$z''_{k+1} = 2\left(\left\lfloor \frac{k+2}{2} \right\rfloor z_{\text{bottom}} - \left\lfloor \frac{k+1}{2} \right\rfloor z_{\text{top}}\right),$$

which prove that (2) and (3) hold. This completes the proof.

As an illustration, **Table 1** provides $z-$coordinates and currents of the image loops up to third order.

Table 1

List of the image loops up to third order for the system presented in Fig. 4.

Loop	$z-$coordinate	Current
Original	0	I
1st order images	$2z_{\text{top}}$ $2z_{\text{bootom}}$	αI
2nd order images	$2(z_{\text{top}} - z_{\text{bootom}})$ $2(z_{\text{bootom}} - z_{\text{top}})$	$\alpha^2 I$
3rd order images	$2(2z_{\text{top}} - z_{\text{bootom}})$ $2(2z_{\text{bootom}} - z_{\text{top}})$	$\alpha^3 I$

Taking into account the images up to kth order, magnetic flux density vector at point $P(x, y, z)$ in the air ($z_{\text{bottom}} < z < z_{\text{top}}$) can be calculated as

$$\vec{\boldsymbol{B}}_K(x, y, z) = \vec{\boldsymbol{B}}(x, y, z) + \sum_{k=1}^{K} \alpha^k \left[\vec{\boldsymbol{B}}(x, y, z - z_k') + \vec{\boldsymbol{B}}(x, y, z - z_k'') \right], \qquad (4)$$

where $\vec{B}(x, y, z)$ denotes magnetic flux density vector generated by the rectangular loop shown in Fig. 1, in homogeneous medium of permeability μ_0. Expressions for the respective components of vector $\vec{\boldsymbol{B}}(x, y, z)$ are provided in Appendix.

If the original loop is placed in the plane $z = z_{lp}$ ($z_{\text{bottom}} < z_{lp} < z_{\text{top}}$), then $z-$coordinates of the images of kth order can be obtained from (2) – (3) by replacing z_k', z_k'', z_{top} and z_{bottom} with $(z_k' - z_{lp})$, $(z_k'' - z_{lp})$, $(z_{\text{top}} - z_{lp})$ and $(z_{\text{bottom}} - z_{lp})$, respectively. For this case, $z-$coordinates of the image loops up to third order are provided in **Table 2**.

Table 2

List of the image loops up to third order when the original loop is placed in the plane $z = z_{lp}$.

Loop	$z-$coordinate	Current
Original	z_{lp}	I
1st order images	$2z_{\text{top}} - z_{lp}$ $2z_{\text{bootom}} - z_{lp}$	αI
2nd order images	$2(z_{\text{top}} - z_{\text{bootom}}) + z_{lp}$ $2(z_{\text{bootom}} - z_{\text{top}}) + z_{lp}$	$\alpha^2 I$
3rd order images	$2(2z_{\text{top}} - z_{\text{bootom}}) - z_{lp}$ $2(2z_{\text{bootom}} - z_{\text{top}}) - z_{lp}$	$\alpha^3 I$

As it was mentioned earlier, the list of the images is infinite. In the following example we investigate the effect of using only finite number of the images. Let us consider configuration presented in Fig. 4, with the rectangular loop having side dimensions $2a = 2b = 20\,\text{cm}$, in the following two cases:

(a) $z_{\text{top}} = 12.5\,\text{cm}$, $z_{\text{bootom}} = -12.5\,\text{cm}$,

(b) $z_{\text{top}} = 20\,\text{cm}$, $z_{\text{bootom}} = -5\,\text{cm}$.

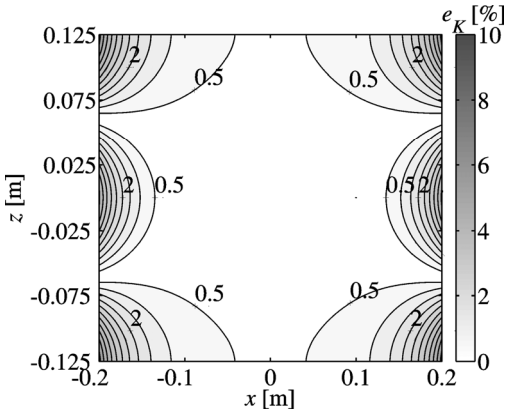

(a)

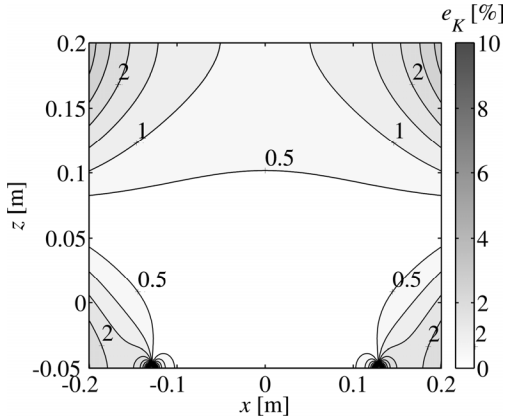

(b)

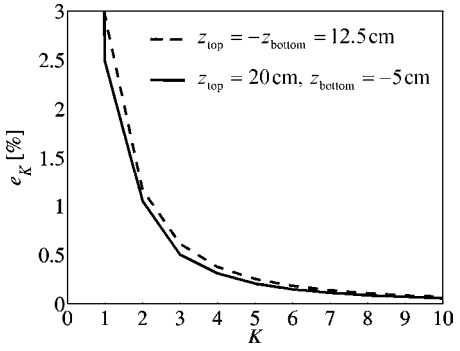

(c)

Fig. 5 – *Relative error* (5) *for* (a) $K = 5,\ z_{top} = -z_{bottom} = 12.5\,cm$ (b) $K = 5,$ $z_{top} = 20\,cm,\ z_{bottom} = -5\,cm,$ (c) *at the origin as a function of* K.

In this example we assume $\mu_r \to \infty$, which according to (1) implies that $\alpha = 1$. Fig. 5 represents relative error defined as

$$e_K[\%] = 100 \cdot \frac{|B_K - B_{\text{ref}}|}{B_{\text{ref}}}, \tag{5}$$

where B_K denotes magnetic flux density magnitude calculated with all images of order up to K and B_{ref} denotes exact value of magnetic flux density magnitude (B_{ref} is calculated for $K = 100$).

Contour-plot of e_K for $K = 5$ in both cases (a) and (b) are presented in Figs. 5a and 5b, respectively. Relative error e_K as a function of K calculated at the center of the original loop (placed at the origin) is presented in Fig. 5c. According to Fig. 5, for most applications, it is sufficient to use images up to fifth order to approximate magnetic field in the air (between blocks).

2.3 Plane of the loop perpendicular to the surfaces of two blocks of high-permeability material

In this subsection we assume that two semi-infinite high-permeability blocks occupy regions $x \le x_{\text{left}} < -a$ and $x \ge x_{\text{right}} > a$, as illustrated in Fig. 6.

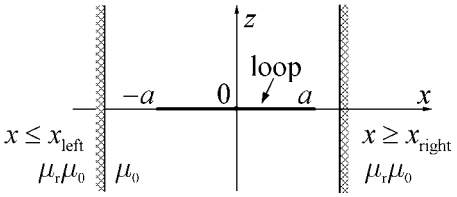

Fig. 6 – *Rectangular loop sandwiched between two blocks* $x \le x_{\text{left}} < -a$ *and* $x \ge x_{\text{right}} > a$.

The following proposition describes the images for the configuration illustrated in Fig. 6.

Proposition 2. For the system presented in Fig. 6, there are two images of nth order, $n \ge 1$, with currents $(-\alpha)^n I$ and centers at $(x'_n, 0, 0)$ and $(x''_n, 0, 0)$, where

$$x'_n = 2\left(\left\lfloor \frac{n+1}{2} \right\rfloor x_{\text{right}} - \left\lfloor \frac{n}{2} \right\rfloor x_{\text{left}} \right), \tag{6}$$

$$x''_n = 2\left(\left\lfloor \frac{n+1}{2} \right\rfloor x_{\text{left}} - \left\lfloor \frac{n}{2} \right\rfloor x_{\text{right}} \right). \tag{7}$$

Proof of Proposition 2 is analogous to the proof of Proposition 1, and it is omitted.

Taking into account the images up to Nth order, the magnetic flux density vector at point $P(x,y,z)$ in the air ($x_{\text{left}} < x < x_{\text{right}}$) can be calculated as

$$\vec{\boldsymbol{B}}_N(x,y,z) = \vec{\boldsymbol{B}}(x,y,z) + \sum_{n=1}^{N}(-\alpha)^n \left[\vec{\boldsymbol{B}}(x-x_n',y,z) + \vec{\boldsymbol{B}}(x-x_n''),y,z \right], \qquad (8)$$

where $\vec{\boldsymbol{B}}(x,y,z)$ denotes magnetic flux density vector generated by the rectangular loop shown in Fig. 1. For expressions of the components of vector $\vec{\boldsymbol{B}}(x,y,z)$ see Appendix.

As an example, we consider configuration presented in Fig. 6, with rectangular loop having side dimensions $2a = 2b = 20\,\text{cm}$. Let us assume $\mu_r \to \infty$, that is $\alpha = 1$ (see (1)), and $x_{\text{right}} = -x_{\text{left}} = 12.5\,\text{cm}$. Relative error e_N (defined analogously as e_K with (5)) as a function of N is presented in Fig. 7. When surfaces of high-permeability blocks are perpendicular to the plane of the original loop, the currents in the image loops of consecutive orders have opposite signs and therefore their effects are partially canceled. As a consequence, the number of images needed to approximate magnetic field for the configuration in Fig. 6 is smaller than the number of images needed when the surfaces of blocks are parallel to the plane of the original loop (as in configuration presented in Fig. 4).

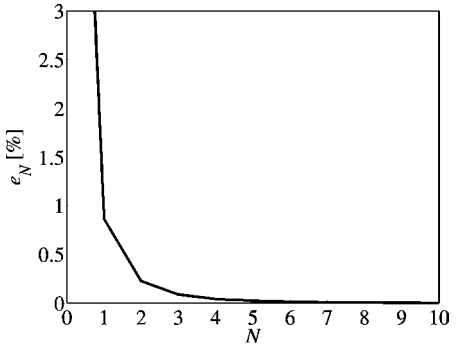

Fig. 7 – *Relative error* e_N.

If the center of the original loop is at the point $(x_{lp},0,0)$, then $x-$coordinates of nth order images can be obtained from (6) – (7) by replacing x_n', x_n'', x_{right} and x_{left} with $(x_n' - x_{lp})$, $(x_n'' - x_{lp})$, $(x_{\text{right}} - x_{lp})$ and $(x_{\text{left}} - x_{lp})$, respectively.

In the case when two semi-infinite high-permeability blocks occupy the regions $y \le y_{\text{back}} < -b$ and $y \ge y_{\text{front}} > b$, the configuration of the system is analogous to the previous one and the corresponding images can be easily determined using the same arguments as in the case when blocks occupy the regions $x \le x_{\text{left}} < -a$ and $x \ge x_{\text{right}} > a$.

3 Case Study: Current Loop Inside High-permeability Cube

In this section application of the method of images to calculation of magnetic field of the rectangular current loop with side dimensions $2a$ by $2a$ placed inside a cube made of high-permeability material is considered. Side dimensions of the cube are $d \times d \times d$ ($d > 2a$).

Let us assume that the center of the current loop and the center of the cube made of high-permeability material coincide. Let us further assume that the plane of the loop is parallel to two surfaces of the cube (placed at $z_{\text{bottom}} = -d/2$ and $z_{\text{top}} = d/2$) and perpendicular to the remaining four surfaces ($x_{\text{left}} = -d/2$, $x_{\text{right}} = d/2$, $y_{\text{back}} = -d/2$ and $y_{\text{front}} = d/2$), as illustrated in Fig. 8.

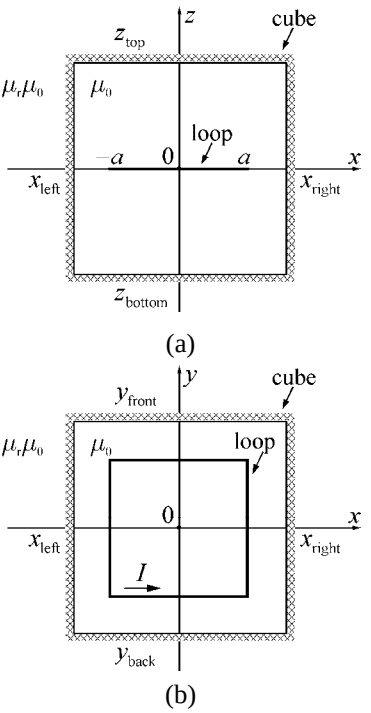

Fig. 8 – *Rectangular loop inside the cube* (a) *side view and* (b) *top view*.

For the loop placed inside the cube made of high-permeability material, it is easy to see that there are $4+2=6$ images of the first order. Since the image of the second order is the "image" of the first order image, it follows that there are $8+2\cdot 4+2=18$ images of the second order. Similarly by continuing this process, we conclude that there are $12+2\cdot(8+4)+2=38$ images of the third order, $16+2\cdot(12+8+4)+2=66$ images of forth order, etc. Thus, there are

$$4l+2\sum_{i=1}^{l-1}4i+2=4l^2+2, \tag{9}$$

images of lth order.

Coordinates of the centers of all 6 image loops of the first order are listed in **Table 3**. Parameter D represents the distance between the center of the corresponding image loop and the origin (center of the original loop).

Table 3

Images of the first order for the loop inside the cube.

Image no.	Coordinates of the center			D	Current
	x	y	z		
1, 2	$\pm d$	0	0	d	$-\alpha I$
3, 4	0	$\pm d$	0	d	$-\alpha I$
5, 6	0	0	$\pm d$	d	αI

List of all images of the second order consists of 18 images (numbered with 7-24) is presented in **Table 4**.

Table 4

Images of the second order for the loop inside the cube.

Image no.	Coordinates of the center			D	Current
	x	y	z		
7, 8	$\pm 2d$	0	0	$2d$	$\alpha^2 I$
9, 10	0	$\pm 2d$	0	$2d$	$\alpha^2 I$
11, 12	0	0	$\pm 2d$	$2d$	$\alpha^2 I$
13-16	$\pm d$	$\pm d$	0	$\sqrt{2}d$	$\alpha^2 I$
17-20	$\pm d$	0	$\pm d$	$\sqrt{2}d$	$-\alpha^2 I$
21-24	0	$\pm d$	$\pm d$	$\sqrt{2}d$	$-\alpha^2 I$

List of all 38 images of the third order is provided in **Table 5**.

Table 5
Images of the third order for the loop inside the cube.

Image no.	Coordinates of the center			D	Current
	x	y	z		
25, 26	$\pm 3d$	0	0	$3d$	$-\alpha^3 I$
27, 28	0	$\pm 3d$	0	$3d$	$-\alpha^3 I$
29, 30	0	0	$\pm 3d$	$3d$	$\alpha^3 I$
31-34	$\pm 2d$	$\pm d$	0	$\sqrt{5}d$	$-\alpha^3 I$
35-38	$\pm 2d$	0	$\pm d$	$\sqrt{5}d$	$\alpha^3 I$
39-42	$\pm d$	$\pm 2d$	0	$\sqrt{5}d$	$-\alpha^3 I$
43-46	$\pm d$	0	$\pm 2d$	$\sqrt{5}d$	$-\alpha^3 I$
47-50	0	$\pm 2d$	$\pm d$	$\sqrt{5}d$	$\alpha^3 I$
51-54	0	$\pm d$	$\pm 2d$	$\sqrt{5}d$	$-\alpha^3 I$
55-62	$\pm d$	$\pm d$	$\pm d$	$\sqrt{3}d$	$\alpha^3 I$

From **Tables 3 – 5** it can be seen that some images of the third order (those numbered with 55-62) are closer to the original loop than images 7 – 12, which belong to the set of images of the second order.

In order to investigate the effects of using only finite number of images, we consider the following six cases

(a) all images of the first order (**Table 3**),
(b) all images up to second order (**Tables 3 – 4**),
(c) all images up to third order (**Tables 3 – 5**),
(d) all images up to forth order (total of 128 images),
(e) all images up to fifth order (total of 230 images),
(f) 122 closest images (all images at distance up to $3d$).

For $\mu_r \to \infty$ and $I = 1\text{A}$, plots of the magnetic flux density magnitude that correspond to the cases listed above are presented in Fig. 9. It can be seen that the calculated values are of oscillatory nature, due to the different algebraic sign of currents in the image loops (see **Tables 3 – 5**). The result converges, but images up to fifth order must be used in order to obtain a good approximation for magnetic field in central region of the cube.

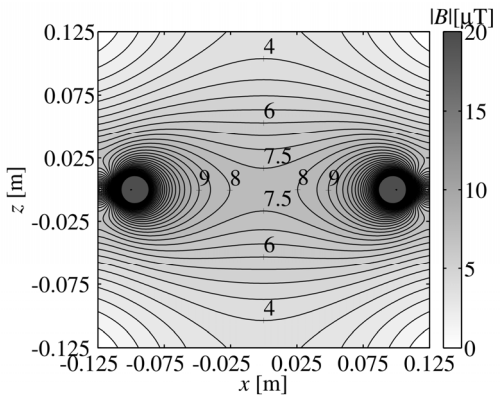

(a)

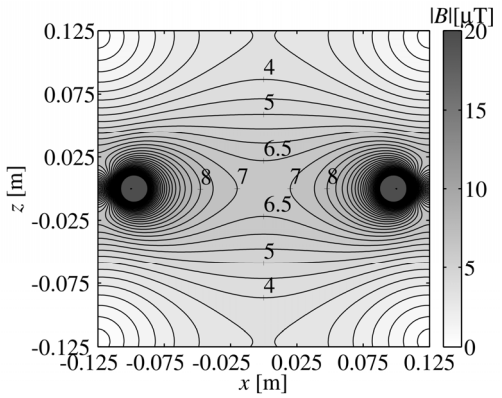

(b)

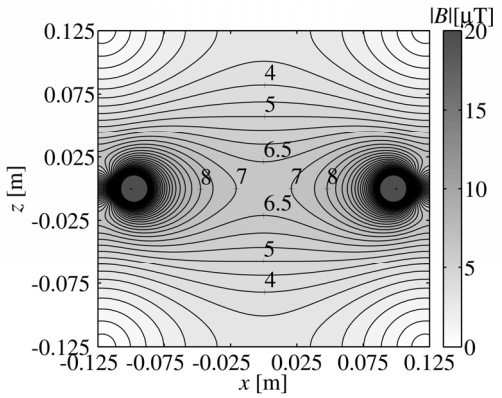

(c)

Fig. 9 – *Magnetic field in the cube calculated with image* (a) *of the 1st order*, (b) *up to 2nd order*, (c) *up to 3rd order*.

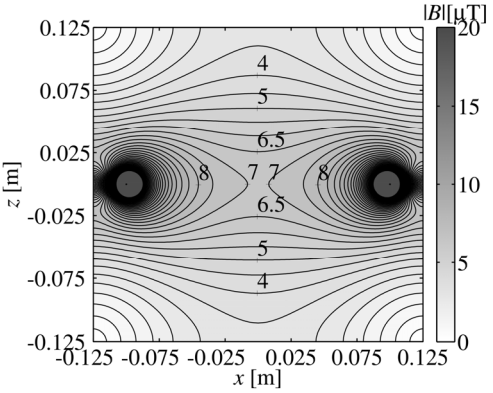

(d)

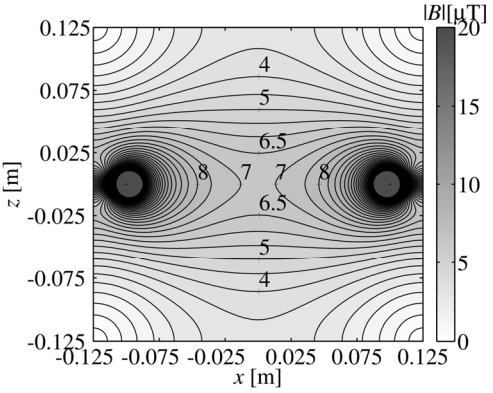

(e)

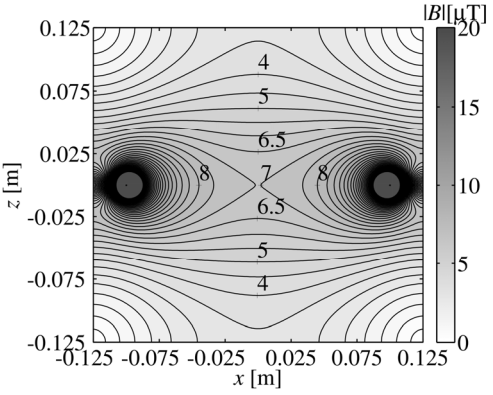

(f)

Fig. 10 – *Magnetic field in the cube calculated with images:* (d) *up to 4th order*, (e) *up to 5th order and* (f) *up to 3d*.

4 Conclusion

In this paper, two cases of the application of the method of current images for calculation of magnetic field of the rectangular loop placed between two semi-infinite blocks of high-permeability material are considered; first when the plane of the loop is parallel to the surfaces of blocks and second when the plane of the loop is perpendicular to the surfaces of blocks. Good approximation for magnetic field between the blocks can be obtained by using ten images (images up to fifth order) in the first case and only four images in the second case (images up to second order). As a case study, the magnetic field of the rectangular loop placed inside the cube made of high-permeability material is also considered.

5 Acknowledgement

This work is supported by Serbian Ministry of Education, Science and Technology Development as a part of the Project TP32016.

6 Appendix

In this appendix, expressions for the components of the magnetic flux density vector of rectangular loop are provided.

For rectangular loop presented in Fig. 1, with side dimensions $2a$ by $2b$, the components of the magnetic flux density vector in free space can be calculated by first considering magnetic vector potential at point with Cartesian coordinates (x, y, z) (see e.g. [10]). The components of magnetic vector potential of the considered loop with current I at point $P(x, y, z)$ can be expressed as:

$$A_x(x,y,z) = \frac{\mu_0 I}{4\pi} \ln\left[\frac{(c_1 + r_1)(c_3 + r_3)}{(c_2 + r_2)(c_4 + r_4)}\right],$$
$$A_y(x,y,z) = \frac{\mu_0 I}{4\pi} \ln\left[\frac{(d_2 + r_2)(d_4 + r_4)}{(d_1 + r_1)(d_3 + r_3)}\right], \tag{1}$$

where

$$\begin{aligned} c_1 &= x + a, & d_1 &= y + b, \\ c_2 &= x - a, & d_2 &= y + b, \\ c_3 &= x - a, & d_3 &= y - b, \\ c_4 &= x + a, & d_4 &= y - b, \end{aligned} \tag{2}$$

and

$$r_i = \sqrt{c_i^2 + d_i^2 + z^2}, \qquad i = 1,\ldots,4. \tag{3}$$

Starting from magnetic vector potential, magnetic flux density vector can be determined by using $\vec{B} = \text{curl}\,\vec{A}$. The components of vector $\vec{B}$ read

$$B_x(x,y,z) = \frac{\mu_0 I}{4\pi}\sum_{k=1}^{4}\frac{(-1)^{k+1} z}{r_k(r_k + d_k)}, \tag{4}$$

$$B_y(x,y,z) = \frac{\mu_0 I}{4\pi}\sum_{k=1}^{4}\frac{(-1)^{k+1} z}{r_k(r_k + c_k)}, \tag{5}$$

$$B_z(x,y,z) = \frac{\mu_0 I}{4\pi}\sum_{k=1}^{4}(-1)^k\left(\frac{c_k}{r_k(r_k + d_k)} + \frac{d_k}{r_k(r_k + c_k)}\right), \tag{6}$$

where c_i, d_i and r_i, $i = 1,\ldots,4$, are defined by (2) – (3). Expressions (4) – (6) can be also obtained starting from Bio-Savart low [11].

The above expressions are derived for the rectangular current loop with the center at the origin and sides parallel to $x-$ and $y-$axis. However, starting from these expressions, it is easy to obtain expressions for the components of magnetic flux density of the loop, parallel to the original loop, with the center at point (x_{lp}, y_{lp}, z_{lp}). In such case, the components of magnetic flux density vector can be obtained from (2) – (6) by replacing x, y and z with $(x - x_{lp})$, $(y - y_{lp})$ and $(z - z_{lp})$, respectively.

7 References

[1] W. Thomson: Reprints of Papers on Electrostatics and Magnetism, 2nd Ed., MacMillan and Co., 1884.

[2] J.C. Maxwell: A Treatise on Electricity and Magnetism, Vol. I, MacMillan and Co., 1873.

[3] P. Hammond: Electric and Magnetic Images, Proceedings of the IEE - Part C: Monograph, Vol. 107, No. 12, Sept. 1960, pp. 306–313.

[4] W.A. Roshen: Planar inductors on magnetic substrates, IEEE Transactions on Magnetics, Vol. 24, No. 6, Nov. 1988, pp. 3213–3216.

[5] W.A. Roshen: Effect of Finite Thickness of Magnetic Substrate on Planar Inductors, IEEE Transactions on Magnetics, Vol. 26, No. 1, Jan. 1990, pp. 270–275.

[6] W.A. Roshen: Analysis of Planar Sandwich Inductors by Current Images, IEEE Transactions on Magnetics, Vol 26, No. 5, Sept. 1990, pp. 2880–2887.

[7] J. Schuderer, W. Oesch, N. Felber, D. Spat, N. Kuster: In Vitro Exposure Apparatus for ELF Magnetic Fields, Bioelectromagnetics, Vol. 25, No.8 , 2004, pp. 582–591.

[8] J.L. Kirschvink: Uniform Magnetic Fields and Double-Wrapped Coil Systems: Improved Techniques for the Design of Bioelectromagnetic Experiments, Bioelectromagnetics, Vol.13, 1992, pp. 401–411.

[9] J. Turowski, M. Turowski: Engineering Electrodynamics: Electric Machine, Transformer, and Power Equipment Design, CRC Press Taylor and Francis Group, 2014.

[10] M. Misakian: Equations for the Magnetic Field Produced by One or More Rectangular Loops of Wire in the Same Plane, Journal of research of the National Institute of Standards and Technology, Vol. 105, No. 4, 2000, pp. 557–564.

[11] D. Herceg, A. Juhas, M. Milutinov: A design of a four square coil system for a biomagnetic experiment, Facta Universitatis, Series: Electronics and Energetics, Vol. 22, No. 3, Dec. 2009, pp. 285–292.